Inorganica Chimica Acta, 128 (1987) 169–173

Kinetics of Imidazole Addition to the Axial Site of the Iron(II) Complex of 2,3,9,10-Tetraphenyl-1,4,8,11-tetraaza-1,3,8,10-cyclotetradecatetraene in Dimethyl Sulfoxide. Evidence for a Dissociative–Interchange Mechanism

SHIGENOBU FUNAHASHI*, NAOTAKA UCHIYAMA, MASAO ISHII and MOTOHARU TANAKA**

Laboratory of Analytical Chemistry, Faculty of Science, Nagoya University, Chikusa, Nagoya 464, Japan

(Received September 3, 1986)

Abstract

The axial adduct formation of the iron(II) complex of 2,3,9,10-tetraphenyl-1,4,8,11-tetraaza-1,3,8,10-cyclotetradecatetraene (L) with imidazole in dimethyl sulfoxide has been investigated spectrophotometrically at various temperatures and pressures. In the presence of a large excess of imidazole the reaction with the two phases has been observed. The first faster reaction is the formation of the monoimidazole complex of FeL^{2+}, and the second slower reaction corresponds to the formation of the bisimidazole complex. Activation parameters are as follows: for the first step with k_1 (25.0 °C) = $(6.8 \pm 0.2) \times 10^5$ mol^{-1} kg s^{-1}, $\Delta H^{\ddagger}_1 = 47.5 \pm 4.9$ kJ mol^{-1}, $\Delta S^{\ddagger}_1 = 26 \pm 16$ J K^{-1} mol^{-1}, and $\Delta V^{\ddagger}_1$ (30.0 °C) = 27.2 ± 1.5 cm^3 mol^{-1}; for the second step with k_2 (25.0 °C) = 26.8 ± 0.8 mol^{-1} kg s^{-1}, $\Delta H^{\ddagger}_2 = 91.6 \pm 0.8$ kJ mol^{-1}, $\Delta S^{\ddagger}_2 = 90 \pm 3$ J K^{-1} mol^{-1}, and $\Delta V^{\ddagger}_2$ (35.0 °C) = 21.8 ± 0.9 cm^3 mol^{-1}. The large positive activation volumes strongly indicate a dissociative character of the activation process.

Introduction

There are a number of kinetic studies on axial ligand substitution reaction in six-coordinated iron(II) complexes with macrocyclic ligands [1]. In the previous paper [1], we have investigated the axial substitution of the iron(II) complex of 2,3,9,10-tetraphenyl-1,4,8,11-tetraaza-1,3,8,10-cyclotetradecatetraene, FeL^{2+} (**1**), with imidazole and thiocyanate ion in acetonitrile. It has been demonstrated that at the higher concentration of imidazole there exists self-associated imidazole which does not react directly with the complex. Since we anticipate that imidazole does not dimerize in dimethyl sulfoxide (Me_2SO) which is much more basic than acetonitrile [2], we have carried out kinetic studies on axial substitution of FeL^{2+} by imidazole in Me_2SO. No report of *trans* effects for axial substitution on the basis of the activation volumes has appeared, although extensive kinetic studies have shown many examples of different lability in axial ligation [3–5]. Herein we also present the pressure effect on the axial substitution.

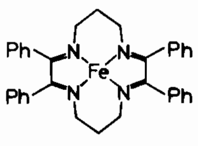

1, FeL^{2+}

Experimental

Material

Reagent grade dimethyl sulfoxide (Wako Pure Chemical Industries, Ltd., Japan) was refluxed over calcium hydride (2 g/dm^3) in an argon atmosphere for more than 3 h, distilled twice under argon, and stored in a dry box. The amount of water contained in Me_2SO used for the kinetic study was found to be less than 6×10^{-3} mol dm^{-3}. Imidazole (Wako) was purified by sublimation under reduced pressure. Preparations of $[FeL(CH_3CN)_2](PF_6)_2$ and anhydrous sodium perchlorate were described previously [1].

Measurements

UV–Vis spectra were measured on a highly sensitive spectrophotometer (Type SM401, Union Giken, Japan). Reaction rates at atmospheric pressure were monitored by a stopped-flow spectrophotometer (Type RA401, Union Giken). Reactions at high pressures were measured with a high-pressure stopped-flow apparatus with spectrophotometric detection (Type FIT-3) [6, 7]. Proton NMR spectra were recorded on an NMR spectrometer (JEOL FX-100).

---

*Adjunct Associate Professor of IMS (1986): Coordination Chemistry Laboratories, Institute for Molecular Science, Okazaki 444, Japan.

**Author to whom correspondence should be addressed.

0020-1693/87/$3.50

© Elsevier Sequoia/Printed in Switzerland

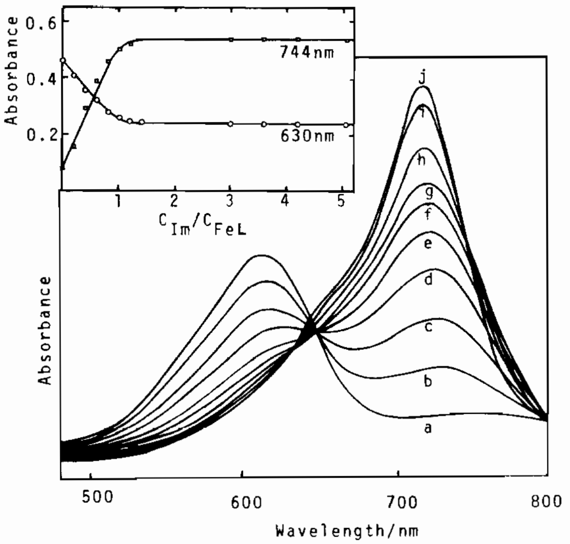

Fig. 1. Visible absorption spectra of FeL^{2+} as a function of the concentration of imidazole. $C_{FeL} = 5.44 \times 10^{-5}$ mol dm^{-3}; C_{Im}/C_{FeL} = 0(a), 0.195(b), 0.405(c), 0.603(d), 0.820(e), 1.02(f), 1.21(g), 2.00(h), 3.00(i), 5.06(j). Inset: Relationship between absorbance and mole ratio.

Results

Equilibria of FeL^{2+} with Imidazole in Me_2SO

Figure 1 shows a series of visible absorption spectra for equilibria of FeL^{2+} with imidazole at various mole ratios of the total concentration of imidazole (C_{Im}) to the total concentration of FeL^{2+} (C_{FeL}) with the constant concentration of FeL^{2+}. The spectra show an isosbestic point at 650 nm until the mole ratio of 0.8 and two isosbestic points at 630 and 744 nm appear at a higher concentration of imidazole ($C_{Im}/C_{FeL} > 1.2$). The absorbance at 630 and 744 nm is plotted against the mole ratio in the inset of Fig. 1. As apparent from the inset, the produced complex over the range of $C_{Im}/C_{FeL} < 1$ should be the 1:1 complex given by eqn. (1).

$$FeL^{2+} + Im \rightleftharpoons FeL(Im)^{2+} \qquad (1)$$

The mole ratio is given by the following equation

$$\frac{C_{Im}}{C_{FeL}} = \frac{1}{C_{FeL}K}\,\frac{\epsilon_1 - \epsilon}{\epsilon - \epsilon_2} + \frac{\epsilon_1 - \epsilon}{\epsilon_1 - \epsilon_2}$$

where ϵ_1 and ϵ_2 are the molar absorption coefficients of FeL^{2+} and $FeL(Im)^{2+}$, respectively and $K = [FeL(Im)^{2+}][FeL^{2+}]^{-1}[Im]^{-1}$ is the formation constant of $FeL(Im)^{2+}$. By using the nonlinear least-squares method, we obtained ϵ_1 (mol^{-1} dm^3 cm^{-1}) = 8.28×10^3 (630 nm), 1.69×10^3 (744 nm), ϵ_2 (mol^{-1} dm^3 cm^{-1}) = 4.35×10^3 (630 nm), 9.98×10^3 (744 nm), and $K = (2.3 \pm 1) \times 10^6$ mol^{-1} dm^3. The curves in the inset of Fig. 1 were depicted by using the obtained values. The absorption spectrum (λ_{max} = 718 nm) of the product produced in the presence of a large excess of imidazole is similar to that of $FeL(Im)_2{}^{2+}$ in acetonitrile. Thus the second step corresponds to the following reaction.

$$FeL(Im)^{2+} + Im \rightleftharpoons FeL(Im)_2{}^{2+} \qquad (2)$$

NMR Spectra

The proton NMR spectrum of $FeL(CH_3CN)_2(PF_6)_2$ in deuterated acetonitrile shows signals at 4.12 and 2.1 ppm which correspond to the α- and β-methylene protons, respectively. Addition of an excess amount of imidazole to this solution produces quantitatively the bisimidazole complex of FeL^{2+} and the methylene signals shift upfield to 3.91 and 1.54 ppm, respectively. On the other hand, for the $FeL(CH_3CN)_2(PF_6)_2$ in Me_2SO-d_6, no methylene proton signal was detectable. However, addition of more than 1 equivalent of imidazole gave the spectrum with the methylene signals at 3.97 and 1.55 ppm which was the same as that of the $FeL(Im)_2{}^{2+}$ in CD_3CN. These findings indicate that FeL^{2+} in CH_3CN is the low-spin diamagnetic complex, while in Me_2SO the FeL^{2+} is the high-spin paramagnetic complex.

Kinetics

Kinetic experiments were carried out at the ionic strength of 0.2 mol kg^{-1} with sodium perchlorate. In the large excess of imidazole we observed the reaction with the two phases. The first faster reaction is the formation reaction of the monoimidazole complex, $FeL(Im)^{2+}$ (reaction 1) and the second slower reaction corresponds to the formation reaction of the bisimidazole complex, $FeL(Im)_2{}^{2+}$ (reaction 2).

In the presence of a large excess of the FeL^{2+} complex over imidazole, only the monoimidazole complex is formed and the bisimidazole complex is not produced. The formation rate of the monoimidazole complex is followed at the absorption maximum of the mono complex of 722 nm. Under the present experimental conditions the reverse reaction can be neglected judging from the formation constant K. The pseudo-first-order plot gave a straight line. Thus the reaction is first-order with respect to imidazole. The rate law is given by eqn. (3).

$$\frac{d[FeL(Im)^{2+}]}{dt} = k_{0(FeL)}[Im] \qquad (3)$$

where $k_{0(FeL)}$ is the conditional first-order rate constant containing the concentration of FeL^{2+}. The plot of $k_{0(FeL)}$ was found to vary linearly with $[FeL^{2+}]$ (see Fig. 2). Therefore, the rate constant is given as $k_{0(FeL)} = k_1[FeL^{2+}]$, where k_1 is the second-order rate constant for reaction 1.

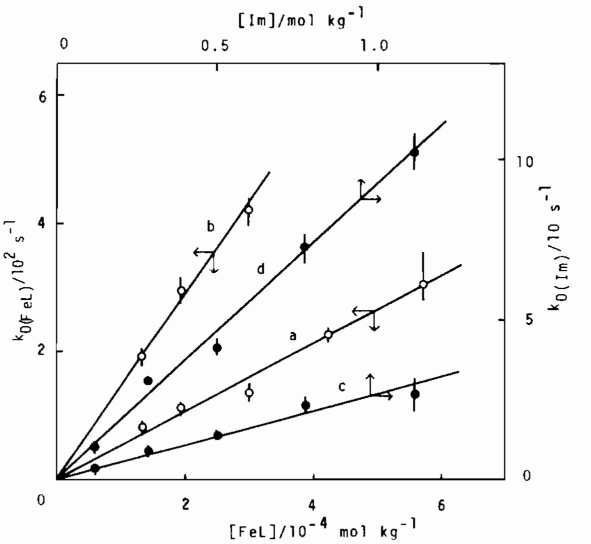

Fig. 2. Concentration dependence of first-order rate constants. Fe(II)L concentration dependence at 20 °C (a) and 35 °C (b); imidazole concentration dependence at 25 °C (c) and 35 °C (d).

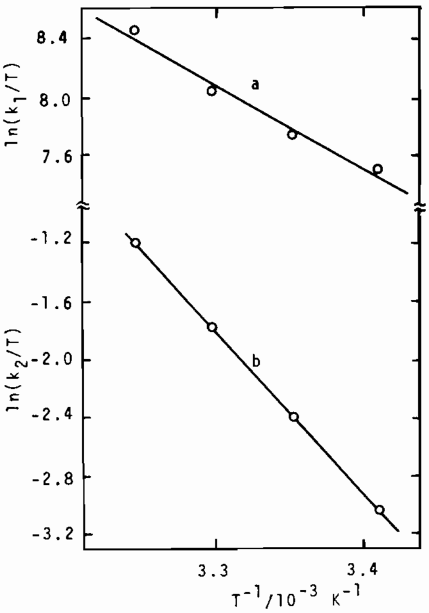

Fig. 3. The Eyring plot. (a) For k_1. (b) For k_2.

The values of k_1 at various temperatures were obtained: k_1 (mol^{-1} kg s^{-1}): $(1.45 \pm 0.03) \times 10^6$ (35 °C), $(9.36 \pm 0.38) \times 10^5$ (30 °C), $(6.83 \pm 0.19) \times 10^5$ (25 °C), $(5.30 \pm 0.13) \times 10^5$ (20 °C), and the Eyring plot is given in Fig. 3a. The enthalpy of activation $\Delta H^{\ddagger}_1$ and the entropy of activation $\Delta S^{\ddagger}_1$ for reaction 1 are 47.5 ± 4.9 kJ mol^{-1} and 26 ± 16 J K^{-1} mol^{-1}, respectively.

Values of k_1 at various pressures are plotted against pressure in Fig. 4a. The relationship between rate constant and pressure is given by the following equation: $(\delta \ln k_1/\delta P)_T = -\Delta V^{\ddagger}_1/RT$. Since, as apparent from Fig. 4a, the plot of $\ln k_1$ against P is linear, the activation volume $\Delta V^{\ddagger}_1$ is independent of pressure. We obtained $\Delta V^{\ddagger}_1 = 27.2 \pm 1.5$ cm^3 mol^{-1} at 30.0 °C.

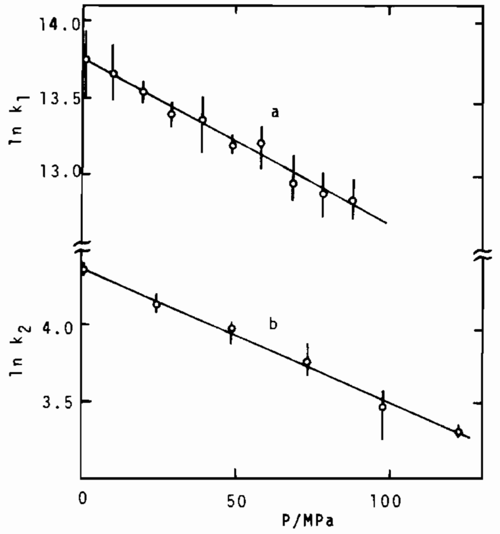

Fig. 4. Pressure dependence of rate constant. (a) For k_1 at 30.0 °C. (b) For k_2 at 35.0 °C.

The rate for formation of the bisimidazole complex was monitored at the maximum absorption wavelength (718 nm) of $FeL(Im)_2^{2+}$ under pseudo-first-order conditions of excess imidazole concentration. After the initial fast reaction, a second, slower reaction was observed. Since the pseudo-first-order plots are excellently linear for more than 3 half-lives, the formation of the bisimidazole complex is first-order with respect to the monoimidazole complex. Thus we have

$$\frac{d[FeL(Im)_2{}^{2+}]}{dt} = k_{0(Im)}[FeL(Im)^{2+}] \tag{4}$$

where $k_{0(Im)}$ is the conditional first-order rate constant involving the concentration of imidazole. The values of $k_{0(Im)}$ at various concentrations of imidazole are plotted against the imidazole concentration in Fig. 2. The plots are linear without intercept. Thus we have $k_{0(Im)} = k_2[Im]$, where k_2 is the second-order rate constant for reaction 2. The k_2 value was obtained from a plot of $k_{0(Im)}$ *versus* [Im] as shown in Fig. 2.

Values of k_2 were obtained at various temperatures and pressures. In Fig. 3b, $\ln(k_2/T)$ is plotted against T^{-1} and in Fig. 4b, the plot of $\ln k_2$ *versus* P at 35.0 °C is given. The enthalpy ($\Delta H^{\ddagger}_2$), entropy ($\Delta S^{\ddagger}_2$), and volume ($\Delta V^{\ddagger}_2$) of activation for reaction 2 were estimated to be 91.6 ± 0.8 kJ mol^{-1}, 90 ± 3 J K^{-1} mol^{-1}, and 21.8 ± 0.9 cm^3 mol^{-1}, respectively.

We also estimated the second-order rate constant in the absence of sodium perchlorate. The rate constant was in good agreement with that obtained at the ionic strength of 0.2 mol kg^{-1} with sodium perchlorate. The absence of any salt effect is consistent with the imidazole reacting as free base.

Discussion

In the reaction of FeL^{2+} with imidazole in acetonitrile, there is a trend of leveling of rates with increasing concentration of imidazole as an incoming ligand [1]. This behavior has been ascribed to the formation of self-associated imidazole at the high concentration of imidazole which is unreactive to the complex. However, in Me_2SO the rates are linearly dependent on the imidazole concentration. Since Me_2SO is much more basic than CH_3CN, the formation of hydrogen-bonded aggregates of imidazole is prevented.

Six-coordinate iron(II) macrocyclic complexes are mostly low spin, but several examples of both five- and six-coordinate high-spin iron(II) complexes with macrocyclic ligands have been reported [14–20]. NMR studies indicate that the iron(II) complex (1) in Me_2SO is high spin, while FeL^{2+} in CH_3CN is low spin. As described in the previous work [1], the rate for addition of imidazole to FeL^{2+} in CH_3CN is very slow in comparison with that for solvent exchange of high-spin iron(II) ion (see Table I). The first imidazole addition is the rate-determining step and the second is not rate limiting. Addition of a large excess of imidazole results in the formation of the six-coordinate bisimidazole complex $FeL(Im)_2^{2+}$. On the other hand, the first step (reaction 1) in Me_2SO is *ca.* 4 orders of magnitude faster than the second step (reaction 2). These facts imply that FeL^{2+} in Me_2SO is high spin, while $FeL(Im)^{2+}$ is low spin. If the high-spin Fe(II)L complex is five coordinate in Me_2SO, the unoccupied sixth coordination site can be attacked by an entering ligand in reaction 1. In such a case, the mechanism should be associative and so negative volume of activation may be expected. However, since a large positive volume of activation (27.2 cm^3 mol^{-1}) was obtained, the FeL^{2+} is the six-coordinate high-spin complex in Me_2SO.

As apparent from the data in Table I, several rate comparisons can be made. Reaction 2 is 4 orders of magnitude slower than reaction 1. The axial substitution reaction in acetonitrile is also as slow as reaction 2. Recently, Butler and Linck [3] have proposed, for axial substitution reactions of $Fe(TIM)X_2^{2+}$ (TIM = 2,3,9,10-tetramethyl-1,4,8,11-tetraazacyclotetradeca-1,3,8,10-tetraene, X = CH_3CN, H_2O, CO), that the much stronger π-accepting ligand in a *trans* position causes a much lower rate of substitution than does the weakly π-accepting ligand. This reduction in rate of substitution at a site *trans* to a strongly π-accepting ligand is consistent with several other studies of low-spin d^6 complexes such as $Fe(DMGH)_2X(py)$ (DMGH = dimethylglyoxime, X = py, benzyl isocyanide) [21], and $Ru(NH_3)_4X(H_2O)^{2+}$ (X = py, CO) [22]. Therefore, it seems reasonable that imidazole and CH_3CN are stronger π-accepting ligands than Me_2SO.

$\Delta H^{\ddagger}$ and $\Delta S^{\ddagger}$ for reaction 1 are very similar to those for solvent Me_2SO exchange on hexakis(dimethyl sulfoxide)iron(II) ion of the high-spin state. On the basis of available volumes of activation for solvent exchange (see Table I), Merbach *et al.* have claimed that solvent exchange reaction of Fe(II) ion proceeds via an interchange mechanism. Unfortunately the activation volume for solvent Me_2SO exchange of Fe(II) ion is not available. In reaction 1, a large positive volume of activation of 27.2 cm^3 mol^{-1} strongly indicates that the reaction is activated by the dissociative mode of activation. Thus the mechanism of reaction 1 is less associative than for simple solvent exchange on solvated iron(II) ion.

The activation volume for reaction 2 is much the same as for reaction 1 although their reaction rates are very different. This reflects a very similar transition state for both reactions. This is reasonable because the large and rigid macrocyclic ligand is blocking the associative attack of an entering ligand to the central metal ion. The activation volume of

TABLE I. Activation Parameters

Reaction system	k (25 °C) (mol^{-1} kg s^{-1})	$\Delta H^{\ddagger}$ (kJ mol^{-1})	$\Delta S^{\ddagger}$ (J K^{-1} mol^{-1})	$\Delta V^{\ddagger}$ (cm^{3}mol^{-1})	Reference
Reaction 1	$(6.8 \pm 0.2) \times 10^5$	47.5 ± 4.9	26 ± 16	27.2 ± 1.5	this work
Reaction 2	26.8 ± 0.8	91.6 ± 0.8	90 ± 3	21.8 ± 0.9	this work
Reaction in CH_3CN[a]	0.69	76 ± 4	7 ± 13	13.7 ± 0.9	1
Me_2SO exchange[b]	1.0×10^6	47.2 ± 2.5	29 ± 8		8
CH_3CN exchange[b]	6.6×10^5	41.4	5.3	3	9, 10
H_2O exchange[b]	4.4×10^6	41.4 ± 1.2	21.2 ± 4.8	3.8 ± 0.2	11
MeOH exchange[b]	5.0×10^4	44.4	13	0.4	12, 13

[a] Formation of the imidazole complex of FeL^{2+} in CH_3CN. [b] Solvent exchange on the hexakis(solvent)iron(II) ion.

13.7 cm^3 mol^{-1} for the reaction in CH_3CN is smaller than that in Me_2SO. An acetonitrile molecule is smaller than an Me_2SO molecule. Thus, the bulkier the solvent molecule, the larger the activation volume.

Acknowledgement

Financial support from the Ministry of Education, Science, and Culture through a Grant-in-Aid for Scientific Research (Grant No. 59430010) and a Grant-in-Aid for Special Project Research (Grant No. 60129031) is gratefully acknowledged.

References

1 S. Funahashi, N. Uchiyama and M. Tanaka, *Bull. Chem. Soc. Jpn., 59*, 161 (1986) and refs. therein.
2 W. C. Barrette Jr., H. W. Johnson Jr. and D. T. Sawyer, *Anal. Chem., 56*, 1890 (1984).
3 A. Butler and R. G. Linck, *Inorg. Chem., 23*, 4545 (1984).
4 D. V. Stynes, K. Singh, B. Ng and S. Wilshire, *Inorg. Chim. Acta, 58*, 179 (1982).
5 F. Pomposo, D. Carruthers and D. V. Stynes, *Inorg. Chem., 21*, 4245 (1982).
6 K. Ishihara, S. Funahashi and M. Tanaka, *Rev. Sci. Instrum., 53*, 1231 (1982).
7 K. Ishihara, S. Funahashi and M. Tanaka, *Inorg. Chem., 22*, 2564 (1983).
8 S. Funahashi and R. B. Jordan, *Inorg. Chem., 16*, 1301 (1977).
9 R. J. West and S. F. Lincoln, *Aust. J. Chem., 24*, 1169 (1971).
10 M. J. Sisley, Y. Yano and T. W. Swaddle, *Inorg. Chem., 21*, 1141 (1982).
11 Y. Ducommun, K. E. Newman and A. E. Merbach, *Inorg. Chem., 19*, 3696 (1980).
12 F. W. Breivogel Jr., *J. Chem. Phys., 51*, 445 (1969).
13 F. K. Meyer, K. E. Newman and A. E. Merbach, *J. Am. Chem. Soc., 101*, 5588 (1979).
14 D. P. Riley, J. A. Stone and D. H. Busch, *J. Am. Chem. Soc., 98*, 1752 (1976).
15 D. C. Olson and J. Vasilevskis, *Inorg. Chem., 11*, 980 (1972).
16 J. C. Dabrowiak and D. H. Busch, *Inorg. Chem., 14* 1881 (1975).
17 D. D. Watkins Jr., D. P. Riley, J. A. Stone and D. H. Busch, *Inorg. Chem., 15*, 387 (1976).
18 J. C. Dabrowiak, P. H. Merrell and D. H. Busch, *Inorg. Chem., 11*, 1979 (1972).
19 V. L. Goedken and D. H. Busch, *J. Am. Chem. Soc., 94*, 7355 (1972).
20 D. P. Riley, P. H. Merrell, J. A. Stone and D. H. Busch, *Inorg. Chem., 14*, 490 (1975).
21 I. W. Pang and D. V. Stynes, *Inorg. Chem., 16*, 590 (1977).
22 S. S. Isied and H. Taube, *Inorg. Chem., 15*, 3070 (1976).